© 2017. Published by The Company of Biologists Ltd | Journal of Experimental Biology (2017) 220, 828-836 doi:10.1242/jeb.139717

RESEARCH ARTICLE

Effects of activation on the elastic properties of intact soleus muscles with a deletion in titin

Jenna A. Monroy[1,*], Krysta L. Powers[2], Cinnamon M. Pace[3], Theodore Uyeno[4] and Kiisa C. Nishikawa[5]

ABSTRACT

Titin has long been known to contribute to muscle passive tension. Recently, it was also demonstrated that titin-based stiffness increases upon Ca^{2+} activation of wild-type mouse psoas myofibrils stretched beyond overlap of the thick and thin filaments. In addition, this increase in titin-based stiffness was impaired in single psoas myofibrils from *mdm* mice, characterized by a deletion in the N2A region of the *Ttn* gene. Here, we investigated the effects of activation on elastic properties of intact soleus muscles from wild-type and *mdm* mice to determine whether titin contributes to active muscle stiffness. Using load-clamp experiments, we compared the stress–strain relationships of elastic elements in active and passive muscles during unloading, and quantified the change in stiffness upon activation. Results from wild-type muscles show that upon activation, the elastic modulus increases, elastic elements develop force at 15% shorter lengths, and there was a 2.9-fold increase in the slope of the stress–strain relationship. These results are qualitatively and quantitatively similar to results from single wild-type psoas myofibrils. In contrast, *mdm* soleus showed no effect of activation on the slope or intercept of the stress–strain relationship, which is consistent with impaired titin activation observed in single *mdm* psoas myofibrils. Therefore, it is likely that titin plays a role in the increase of active muscle stiffness during rapid unloading. These results are consistent with the idea that, in addition to the thin filaments, titin is activated upon Ca^{2+} influx in skeletal muscle.

KEY WORDS: Titin, Connectin, Muscle activation, Muscular dystrophy with myositis (*mdm*), Elastic recoil

INTRODUCTION

Muscle stiffness increases ∼3-fold from the passive state to maximum isometric force (Campbell and Moss, 2002). When muscles are activated, an increase in muscle stiffness can be measured even before the cross-bridges begin to produce force, suggesting that a non-cross-bridge element contributes to the increased muscle stiffness (Bagni et al., 2002, 2004; Rassier et al., 2015). Although titin has long been thought to contribute to muscle passive tension (Maruyama, 1976; Magid and Law, 1985; Wang et al., 1991; Linke et al., 1998), a role for titin in active muscle has increasingly been proposed (Tatsumi et al., 2001; Bagni et al., 2002; Herzog and Leonard, 2002; Leonard and Herzog, 2010; Lindstedt et al., 2002; Nishikawa et al., 2012; Rassier et al., 2015; Herzog et al., 2016; Rivas-Pardo et al., 2016). Recent work on single myofibrils stretched beyond overlap of the thick and thin filaments clearly demonstrates that titin-based stiffness increases upon Ca^{2+} activation (Leonard and Herzog, 2010; Powers et al., 2014, 2016). The goal of the present study is to further investigate whether titin contributes to active stiffness of intact soleus muscles by measuring elastic recoil during rapid unloading tests.

Here, we used load-clamp experiments to compare the elastic recoil of passive and activated muscles during rapid unloading. Active muscles shorten biphasically in response to a rapid decrease in load (Wilkie, 1956; Jewell and Wilkie, 1958; Lappin et al., 2006). The initial fast phase of shortening has been attributed to elastic elements, whereas the slow phase of shortening is due to cycling of the cross-bridges (Wilkie, 1956; Jewell and Wilkie, 1958). We took advantage of the load-clamp test to measure the elastic properties of intact muscles by estimating the stress–strain relationship of the elastic elements during rapid unloading in active and passive muscle. This allowed us to quantify the change in stiffness of elastic elements in muscle as a result of activation.

Intact skeletal muscles are composed of a variety of elastic elements, both inside and outside muscle sarcomeres (Gindre et al., 2013; Roberts, 2016). Owing to the complexity and integration of these structures, it is difficult to differentiate their roles at the level of intact muscles. By comparing rapid unloading of passive and active muscles, we can measure the change in stiffness of elastic elements that occurs upon activation. We predicted that the stress–strain relationship of intact soleus muscles during rapid unloading would shift leftward upon activation in wild-type muscles, indicating that elastic structures in active muscles are stiffer. Thus, for a given change in load, active muscles should recoil less than passive muscles.

To investigate whether titin plays a role in increasing muscle stiffness during activation, we used the muscular dystrophy with myositis (*mdm*) mouse, which is characterized by a 779 bp deletion in the N2A region of the *Ttn* gene (Garvey et al., 2002). As a result of this deletion, the *mdm* mouse exhibits low muscle forces and an impaired walking gait (Huebsch et al., 2005; Lopez et al., 2008). Powers et al. (2016) recently demonstrated that single psoas myofibrils from *mdm* muscles fail to show an increase in titin-based stiffness upon activation when stretched beyond overlap of the thick and thin filaments. Thus, we predicted that there would be no shift in the stress–strain relationship of intact *mdm* soleus muscles upon activation.

We designed load-clamp experiments to measure elastic recoil of intact wild-type and *mdm* soleus muscles during rapid unloading to provide additional insight into the relative contributions of elastic elements inside and outside muscle sarcomeres to active muscle stiffness. By matching the initial stress and the change in stress for

[1]W. M. Keck Science Department, The Claremont Colleges, Claremont, CA 91711, USA. [2]Human Performance Laboratory, Department of Kinesiology, University of Calgary, Calgary, AB, Canada T2N 1N4. [3]Department of Biological Sciences, LeMoyne College, Syracuse, NY 13214, USA. [4]Department of Biology, Valdosta State University, Valdosta, GA 31698, USA. [5]Center for Bioengineering Innovation and Department of Biological Sciences, Northern Arizona University, Flagstaff, AZ 86011, USA.

*Author for correspondence (jenna.monroy@gmail.com)

J.A.M., 0000-0001-7635-8613

Received 9 March 2016; Accepted 12 December 2016

Journal of Experimental Biology

Journal of Experimental Biology (2017) 220, 828-836 doi:10.1242/jeb.139717

Symbols and abbreviations

CSA	cross-sectional area
d	constant describing muscle stiffness
F	force
F_o	initial force
HSD	honestly significant difference
Ig	immunoglobulin-like domains of titin
L	muscle length
L_0	optimal muscle length
L_f	muscle fiber length
mdm	muscular dystrophy with myositis mutation
N2A	region of titin between tandem Ig and PEVK domains
P_0	maximum isometric force
PEVK	domain rich in proline (P), glutamate (E), valine (V) and lysine (E)
r	Pearson product–moment correlation coefficient
Ttn	titin gene
V_{max}	maximum contraction velocity
x	muscle strain during rapid unloading

each muscle in active and passive load-clamp tests, the recoil of linear series elastic elements outside the sarcomere was held constant. We conducted active load-clamp tests at two lengths along the length–tension curve [85% optimum muscle length (L_0) and L_0] to quantify the contribution of elastic elements outside muscle sarcomeres to active muscle stiffness. On the ascending limb of the length–tension relationship (85% L_0), elastic elements in mouse soleus muscles are slack (Berquin et al., 1994) and therefore should not contribute to the increase in muscle stiffness with activation. The contribution, if any, of extrinsic elastic elements to muscle stiffness during rapid unloading should be smaller on the ascending limb than at optimal length. If active muscle stiffness increases owing to stretch of extrinsic elastic elements, then the unloaded force–length curve should shift leftward as initial muscle length increases. If no difference in active muscle stiffness is found between 85% L_0 and L_0, this would suggest that elastic elements outside muscle sarcomeres contribute negligibly to active muscle stiffness at these lengths.

MATERIALS AND METHODS

Animals

Heterozygous mice of the strain B6C3Fe a/a-Ttn^{mdm}/J were obtained from the Jackson Laboratory (Bar Harbor, ME, USA). A breeding colony was established to obtain wild-type and homozygous recessive mice (*mdm*). Heterozygous and wild-type littermates were identified using PCR analysis of tail snips using the following primers: 5′-GGAGTGACTGAACAATGAACG-3′ (Ttn55F, forward) and 5′-GACCAGACTGGAATTCTAAGG-3′ (Ttn55R, reverse) for wild type, and 5′-AGGACCAACAGAGCT-GACTG-3′ (Ttn58F, forward) and 5′-CCTCTTTTCCAATTTGA-GGC-3′ (mdm1R, reverse) for *mdm* (Garvey et al., 2002; Lopez et al., 2008). Experiments were conducted on 10 wild-type and 10 *mdm* soleus muscles of age-matched mice (mean±s.e.m. wild-type age=41.9±12.8 days; mean±s.e.m. *mdm* age=42.4±12.7 days; range=32–73 days). The Institutional Animal Care and Use Committee at Northern Arizona University approved the experimental protocol and use of these animals.

Muscle preparation

Mice were anesthetized with 1–2% isoflurane mixed with oxygen delivered at 1–1.5 l min^{-1} and euthanized immediately following muscle extraction. The soleus muscles from both limbs were dissected from each mouse. Using 4-0 silk suture, the muscles were tied off securely at the muscle–tendon junction to minimize the contribution of extramuscular connective tissue to the experiments. Muscles were immersed in a mammalian Krebs–Ringer bath (in mmol l^{-1}: 137 NaCl, 5 KCl, 1 NaH_2PO_4, 24 $NaHCO_3$, 2 $CaCl_2$, 1 $MgSO_4$ and 11 dextrose, pH 7.4), buffered with 95% O_2 and 5% CO_2, and maintained at room temperature (23–25°C). At this temperature, muscles remain healthy and the maximum tetanic force remains stable for several hours. The maximum isometric stress at room temperature is 90% of the maximum isometric stress at the normal body temperature of 37°C (James et al., 2015). The distal end of the muscle was attached to an inflexible hook and the proximal end was attached to a dual servomotor force lever (Aurora Scientific, Inc., Series 300B, Aurora, ON, Canada) that measured position and force.

Data collection

Contractile and elastic properties were measured *in vitro* from soleus muscles dissected from *mdm* and wild-type littermates. Muscle length was adjusted so that the soleus was taut and the passive tension was 0.002–0.005 N. Using digital calipers, muscle length was measured from the origin to the myotendinous junction. Muscles were stimulated using an electrical field generated between two platinum electrodes connected to a Grass S48 stimulator. Muscles were activated using a 1 ms square pulse at supramaximal intensity. To determine L_0, muscle length was adjusted until a single pulse elicited maximum twitch force. Pulse trains of 800–1000 ms at a stimulus frequency of 70–75 Hz were delivered to the muscles to obtain maximum isometric force (P_0). Maximum isometric force was maintained throughout all the experiments. Muscles that experienced >10% drop in force during an experiment were removed from the analysis.

After testing, the Achilles tendon and femoral tendinous origin were removed, and the muscle was dabbed dry and weighed. Maximum isometric stress (N cm^{-2}) was determined by dividing P_0 by physiological cross-sectional area (CSA). To determine CSA, muscle mass was multiplied by the cosine of the pennation angle (8.5 deg; Burkholder et al., 1994), and divided by the product of muscle fiber length (L_f) and the density of mammalian skeletal muscle (1.06 g cm^{-3}; Sacks and Roy, 1982). Fiber length (L_f) was determined using nitric acid digestion (Maxwell et al., 1974). Three muscles from each genotype were fixed at L_0 in 10% formalin for 24 h and immersed in 20% HNO_3 to digest surrounding connective tissue. Following digestion, the muscles were kept in 50% glycerol. Single fibers were teased from the muscles and at least 10 fibers per muscle were measured for each genotype. The mean fiber length/muscle length ratios did not differ between genotypes (means±s.e.m.; wild-type=0.80±0.05, *mdm*=0.81±0.05; P=0.88) and were similar to ratios reported in the literature (Burkholder and Lieber, 2001; Askew and Marsh, 1997). A mean value of 0.8 was used for all muscles.

Elastic properties

A series of load-clamp experiments was used to compare active and passive elastic recoil between wild-type and *mdm* soleus muscles (Fig. 1). During load-clamp experiments, muscles are rapidly unloaded while the change in muscle length is recorded. When the load is reduced, muscles shorten biphasically, with an initial rapid change in length owing to recoil of elastic elements and a later slow phase due to cross-bridge cycling (Wilkie, 1956; Jewell and Wilkie, 1958; Lappin et al., 2006; Monroy et al., 2007). For each muscle, the initial stress and change in stress were matched for load-clamps in the active and passive states (Fig. 1, upper panels). A range of initial

Journal of Experimental Biology (2017) 220, 828-836 doi:10.1242/jeb.139717

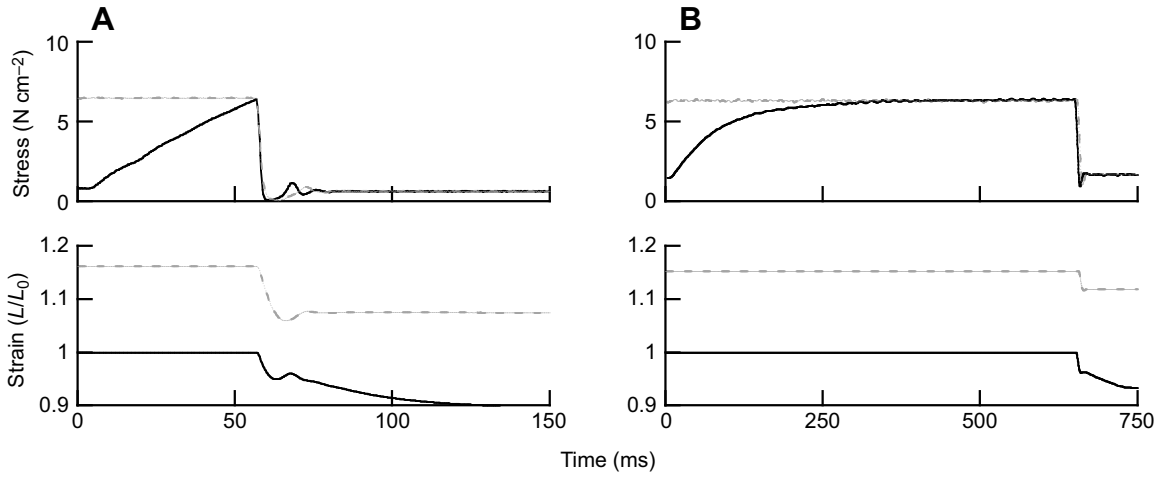

Fig. 1. Passive and active loadclamp experiments from representative wild-type and *mdm* soleus muscles. Top: the muscles were stretched passively (dotted gray line) or activated (solid black line) to the same initial stress, after which the stress was reduced by the same amount. To match stresses, wild-type muscles (A) were activated to 30–50% P_0 whereas *mdm* muscles (B) were activated to 100% P_0. Bottom: in both the active and passive states, muscles recoiled elastically during rapid unloading. The ratio of the initial change in muscle length to the starting length, i.e. strain, was measured in response to the rapid decrease in stress. Note that the active muscles continue to shorten following elastic recoil as a result of interaction of the contractile proteins.

stresses was chosen to determine the effect of initial stress on elastic recoil. For active load clamps, muscles were stimulated tetanically to achieve forces ranging from 10–100% P_0, followed by rapid step-decreases in load (2–95% P_0). The duration of stimulation was varied to achieve different initial stresses.

For passive load clamps, muscles were stretched to a length at which the initial steady-state passive stress equaled the active stress, after which the load was reduced using the same step-decreases as in the active experiments. *mdm* muscles (n=10) were stretched until the passive force ranged from 30–100% P_0. Because active force (P_0) is low and passive force is high in *mdm* muscles, passive force could be matched with active force even at 100% P_0. Depending on the initial force, passive *mdm* muscles were stretched to 1.02–1.14 L_0. Passive wild-type muscles were stretched until the passive stress was equal to the passive stress of mutant muscles. Wild-type muscles (n=10) were stretched until the passive force ranged from 10–30% P_0 and 1.09–1.17 L_0. Although the longest stretches are somewhat beyond the *in vivo* sarcomere length operating range (Goulding et al., 1997), the goal of the experiment was to unload the passive and active muscles from the same starting and ending forces.

Active load-clamp tests were performed at two lengths (85% L_0 and L_0) along the length–tension relationship to quantify the contribution of elastic elements outside the sarcomere to active muscle stiffness (n=4 wild type, n=4 *mdm*). The initial stress and change in stress were matched for load-clamp tests at each length. Muscles were stimulated tetanically to achieve the same initial stress, followed by rapid step-decreases in load (2–95% P_0). The duration of stimulation was varied to achieve different initial stresses.

For active and passive load-clamp trials, the initial rapid change in length (mm, L/L_0) was measured (Fig. 1, lower panels) (Lappin et al., 2006). Briefly, the slope and intercept of the line that represents the slow phase shortening velocity was determined. This line was extrapolated to the y-intercept (t=0) and the end of the initial rapid phase was defined as the intersection of this line and the observed change in muscle length versus time (Lappin et al., 2006). For each muscle in each state (passive versus active), data from 6–8 load clamp tests were collected to model the stress–strain relationship. Custom software (LabVIEW 7.1, National Instruments, Austin, TX, USA) controlled servomotor parameters and recorded data from the force lever system. The data were sampled at 4000 Hz.

Modeling muscles as exponential springs

When an exponential spring is unloaded (Fig. 2A), there is a logarithmic relationship between the change in stress and the change in strain (Fig. 2B). For a given change in stress, muscles recoil farther when the initial stress is lower (compare red versus green lines in Fig. 2B). A similar logarithmic relationship is observed during rapid unloading of skeletal muscle. When the change in load is small, muscles recoil a short distance and when the change in load is large, muscles recoil a disproportionately greater distance (Lappin et al., 2006). Muscles activated to lower initial forces recoil greater distances for a given change in load and thus, are more compliant. Therefore, the stress–strain relationship of the elastic elements in muscle was modeled as an exponential spring (Eqn 1):

$$\text{Force} = F_0(e^{x/d} - 1). \quad (1)$$

MATLAB (MathWorks) was used to find the parameters F_0 and d that best predicted the observed elastic recoil data collected from each muscle in load-clamp tests. The value of the constant F_0 did not vary

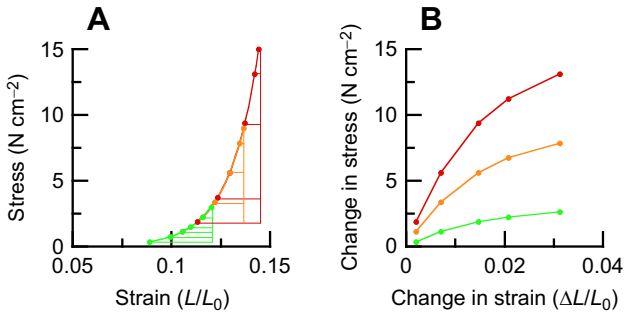

Fig. 2. Theoretical exponential spring. Theoretical exponential spring was calculated as $F=F_0(e^{(x/d)}-1)$, with F=stress, x=strain, and constants F_0 and d. (A) Each color represents a series of load-clamp experiments (n=5) from three initial stresses, 15 N cm^{-2} (red); 9 N cm^{-2} (orange); 3 N cm^{-2} (green). (B) Change in stress versus change in strain for each load-clamp experiment. For a given change in stress, the change in strain is greater when the initial stress is lower. For a given change in strain, the change in stress is greater when the initial stress is greater. A leftward shift in the stress–strain relationship of an exponential spring would result in a smaller change in strain for a given change in stress for all initial stresses.

Journal of Experimental Biology

Journal of Experimental Biology (2017) 220, 828-836 doi:10.1242/jeb.139717

among muscles. This value was held at 0.0001 for all normalized data and 0.00001 for raw data. The value of the constant d describes the shape of the unloading curve, and x describes strain. Because Young's modulus of elasticity is defined as the initial slope of the stress–strain curve, the constant d describes how the elastic modulus changes with muscle stress, with greater d values corresponding to greater compliance (lower elastic modulus) during elastic recoil. The elastic modulus (Eqn 2) is the derivative of Eqn 1:

$$\text{Elastic modulus} = F_0 e^{x/d}/d. \quad (2)$$

The exponential model (Eqn 1) fit the observed muscle data when the change in load was between 10% and 95% of the initial force. For this range of initial forces, the model explained most of the variance in observed length changes in active (r^2=0.93±0.007) and passive wild-type muscles (r^2=0.86±0.01), as well as active (r^2=0.88±0.01) and passive (r^2=0.8±0.03) *mdm* muscles.

Because silk suture exhibits some compliance, we also modeled the behavior of the 4-0 silk suture used to attach the muscle to the force lever in order to account for its contribution to the total displacement during the load-clamp experiments. We performed load-clamp experiments on two pieces of silk suture tied to the ends of an inextensible piece of metal with a length equal to the average muscle length (10 mm). The suture pieces were equal in length to the average length of the suture used during muscle experiments. The suture preparation was stretched until a steady-state force matched the muscle experiments, after which the load was reduced and the change in length was measured as described above. A series of six step-decreases in load were recorded for each of five initial steady-state forces (0.007-0.07 N), the range of which corresponded to the muscle experiments. Using MATLAB, we obtained the parameters F_0 and d that best described the relationship between force and length. The value of the constant F_0 was 0.0001 for all trials. In contrast to muscle, the value of d did not vary with initial force (r=−0.3959; P=0.51). Therefore, an exponential function with a single d-value (d=5.4×10^{-5}) was used to fit the data from all the suture load-clamp trials. The analysis showed a strong relationship (r^2=0.98) between the change in length of the suture predicted by the function and the observed change in length from the experiments. Using Eqn 1, we subtracted the contribution of the suture from all of the load-clamp trials. The suture contributed from 8% to 63% to the total displacement. When the initial force and change in load was small (<5%), suture contributed up to 63% of the total displacement. However, when the change in load was larger (5–95% P_0), the suture contributed only 8–10% of the total displacement. After removing the suture contribution, we modeled the elastic behavior of the muscle.

Statistics

One-way ANOVA was used to compare active tension between genotypes. Passive stress was log-transformed to linearize passive stress–strain data. ANCOVA, with genotype (*mdm*, wild-type) as the main effect, individual as a random effect nested within genotype, and strain (L/L_0) as the covariate, was used to compare log-transformed passive stress–strain data between genotypes. Similarly, active and passive stress during rapid unloading were log-transformed and ANCOVA, with muscle state (passive, active) and genotype (*mdm*, wild-type) as the main effects, individual as a random effect nested within genotype, and muscle stress as the covariate, was used to compare the stress–strain relationship during rapid unloading. The x-intercepts and elastic modulus were compared among states and genotypes. Because there was a significant interaction between genotype and state, Tukey's HSD test was used to determine the relationships among the muscle states and genotypes.

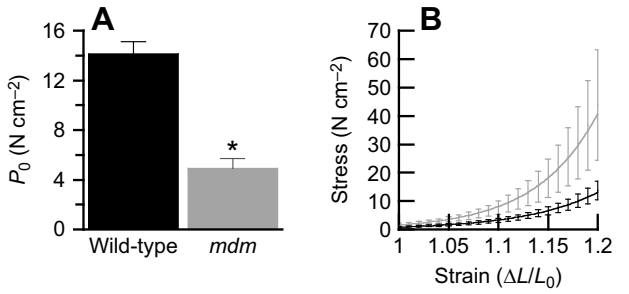

Fig. 3. Contractile and passive properties of wild-type and *mdm* soleus muscles. (A) The maximum active stress (P_0) is greater in wild-type (black, n=10) compared with *mdm* (gray, n=10) muscles (ANOVA, *P<0.0001). (B) Passive stress, depicted as log-transformed passive stress–strain relationship, is greater in *mdm* compared with wild-type muscles (ANCOVA, P<0.01). Data presented as means±s.e.m.

RESULTS

The maximum isometric stress of wild-type soleus muscles was significantly greater than for *mdm* soleus (ANOVA, P<0.0001; Fig. 3A). The slope of the log-transformed passive stress–strain relationship was significantly greater for *mdm* muscles, indicating greater passive stiffness (ANCOVA, P=0.01; Fig. 3B).

Passively stretched wild-type muscles shortened farther than when the muscles were activated to the same initial stress followed by the same decrease in load, indicating that the stiffness of elastic elements increased with activation (Fig. 4A). Activation caused a leftward shift of the stress–strain relationship during unloading in wild-type (Fig. 4B) but not *mdm* muscles (Fig. 4C,D). The slope of the log-transformed stress–strain relationship increased 2.9-fold

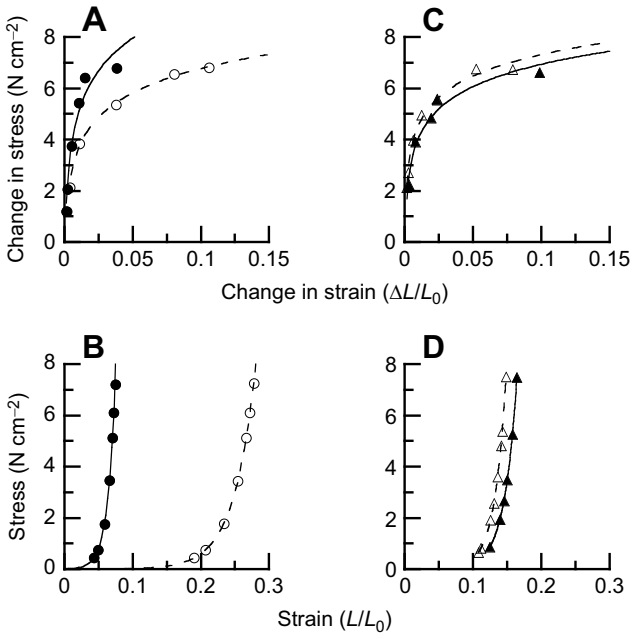

Fig. 4. Change in stress versus change in strain. (A,C) Change in stress versus change in strain for activated (solid symbols) and passively stretched (open symbols) wild-type (A) and *mdm* (C) soleus at the same initial stress. (B,D) Stress–strain curves for wild-type muscle depicted in A (B) and *mdm* muscle depicted in C (D).

Journal of Experimental Biology (2017) 220, 828-836 doi:10.1242/jeb.139717

in wild-type muscles (Fig. 5), from 16.2 to 47.4 upon activation (ANCOVA, P=0.003). There was no difference in slope (active=33.2; passive=26.1) of the log-transformed stress–strain relationship upon activation in *mdm* soleus (ANCOVA, P=0.17).

The x-intercepts of the log-transformed stress–strain relationship during unloading (Fig. 5) represent the muscle lengths at which tension develops (i.e. resting length) in elastic elements. In general, the intercepts of the stress–strain relationships were more variable for the passive than for the active wild-type muscles (Fig. 5A). In active wild-type soleus, tension in elastic elements developed at a length that was 15.0±1.2% shorter than in passive muscles (paired t-test, P<0.0001; Fig. 5A). In *mdm* soleus, both passive and active stress–strain relationships were variable (Fig. 5B) and there was no significant difference (2.8±1.4%) in the x-intercepts between the active and passive states (paired t-test, P=0.07; Fig. 5B).

When activated to the same initial stress at 85% L_0 and L_0, wild-type soleus muscles shortened by the same distance in response to the same decrease in load, indicating that there was no difference in active muscle stiffness between muscles on the ascending limb and at L_0 on the length–tension curve (Fig. 6A). There was no effect of muscle length on the slopes (85% L_0=39.7; L_0=41.3) of the log-transformed stress–strain relationship, indicating no change in the elastic modulus with increasing muscle length (ANCOVA, P=0.2; Fig. 6B). In *mdm* soleus, there was no significant difference in the x-intercepts between the two lengths (paired t-test, P=0.56; Fig. 6C, D). Because the initial forces were difficult to match at 85% L_0 and L_0, the active stress–strain relationship at L_0 shifted leftward in two of the four *mdm* muscles. Thus, there was a nearly significant difference in the slopes of the log-transformed stress–strain relationship (ANCOVA, P=0.051). In the two muscles, there was no effect of length on elastic recoil. In the other two muscles, there was a leftward shift of activated muscles starting at L_0, which was most likely due to the variation in initial forces between trials.

During unloading, the Young's modulus of elasticity increased linearly with muscle stress (ANCOVA, P<0.0001; Fig. 7). There was also a significant genotype by state (active versus passive) effect on the Young's modulus (ANCOVA, P<0.0001). A Tukey's HSD test showed that the elastic modulus was greatest for active wild-type muscles and smallest for passive wild-type muscles, with active and passive *mdm* muscles falling between these values. The slope of the elastic modulus–stress relationship increased from 41.0x to 109.3x, a factor of 2.7, when wild-type muscles were activated (ANCOVA, P=0.001). For the *mdm* soleus, the difference in slope of the Young's modulus–stress relationship between passive (64.9x) and active (75.3x) muscles was not statistically significant (ANCOVA, P=0.57).

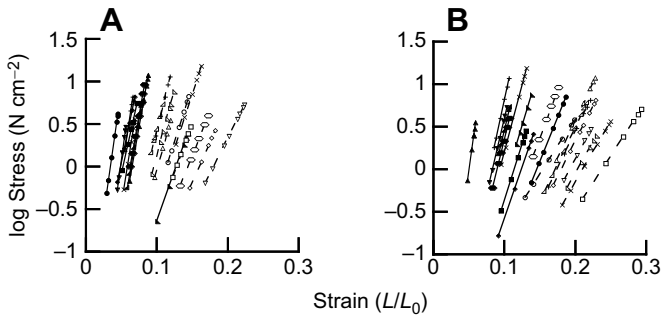

Fig. 5. Log transformed stress–strain relationship during rapid unloading. Activated (filled symbols, solid line) and passively stretched (open symbols, dashed line) (A) wild-type and (B) *mdm* soleus. In wild-type muscles, elastic elements developed tension at 15.0% shorter lengths when activated (paired t-test, P<0.0001). There was no significant difference in the x-intercepts between the active and passive *mdm* soleus (paired t-test, P=0.07).

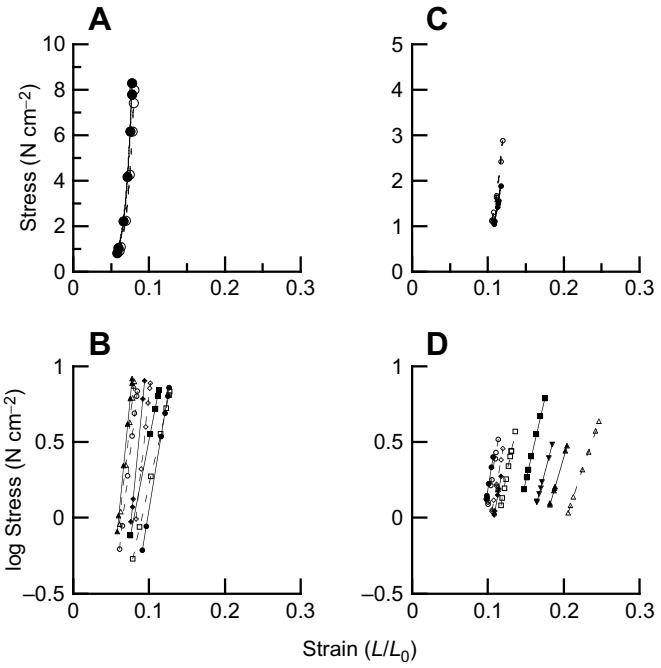

Fig. 6. Stress–strain curves at different initial lengths. (A,C) Wild-type (A) and *mdm* (C) soleus muscle activated to the same initial stress at L_0 (open symbols, dashed line) and 85% L_0 (closed symbols, solid line). (B,D) Log transformed stress–strain relationship for wild-type (B) and *mdm* (D) soleus muscles activated at L_0 and activated at 85% L_0. There was no effect of starting length (85% L_0, L_0) on the slope of the log-transformed stress–strain relationship of activated wild-type soleus (ANCOVA, P=0.2, n=4). There was a nearly significant effect of starting length on the stress–strain relationship of activated *mdm* muscles (ANCOVA, P=0.051, n=5).

DISCUSSION

Our results show that the Young's modulus of elastic elements that recoil during rapid unloading increases upon activation in soleus muscles from wild-type mice. When wild-type soleus muscles were activated, there was a leftward shift (less deformation for a given

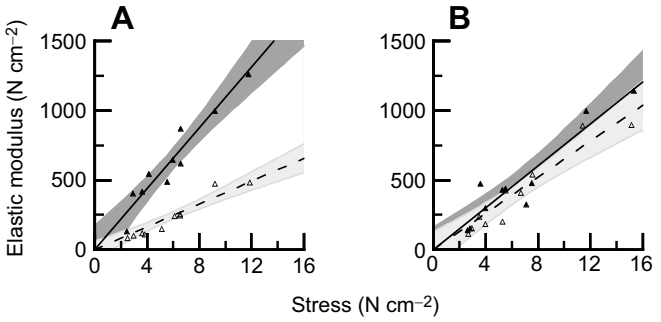

Fig. 7. Elastic modulus versus stress. The relationship between elastic modulus and stress is depicted. (A) Active (closed symbols, solid line, y=109.3x) and passive (open symbols, dashed line, y=41.0x) wild-type muscles. (B) Active (closed symbols, solid line, y=75.3x) and passive (open symbols, dashed line, y=64.9x) *mdm* muscles. A Tukey's HSD test (α=0.05) showed that the elastic modulus was greatest for active wild-type muscles and smallest for passive wild-type muscles (A), with active and passive *mdm* muscles falling between these values (B). Shaded areas indicate 95% confidence intervals (activated, dark gray; passive, light gray).

Journal of Experimental Biology

Journal of Experimental Biology (2017) 220, 828-836 doi:10.1242/jeb.139717

load) of the stress–strain relationship. During rapid unloading, elastic elements of active wild-type muscles began to develop force at lengths that were 15% shorter than in passive muscles, and upon activation there was a 2.7-fold increase in the slope of the elastic modulus versus stress. In contrast, there was no change in the stress–strain relationship and no change in the resting length of elastic elements during rapid unloading in *mdm* soleus.

Comparison with other studies

We observed that the length at which soleus muscles begin to develop force (i.e. resting length) changes by ∼15% upon activation. This result is consistent with Lappin et al. (2006), who observed that toad muscles recoil elastically by ∼20% of their length upon activation at L_0. These large strains in elastic elements of active muscle are too large to be borne by the cross-bridges or filament lattice of the sarcomeres alone (Lappin et al., 2006). Similarly, although single fibers from the telson muscle of horseshoe crabs recoil by only 6% during rapid unloading, they shorten by 210 nm per half-sarcomere owing to the extreme length of the sarcomeres (Akimoto and Sugi, 1999). The inference from these observations is that the elastic titin protein likely contributes to active elastic recoil in these muscles (Sugi et al., 2000; Lappin et al., 2006).

Powers et al. (2014) stretched single myofibrils from wild-type mouse psoas beyond overlap of the thick and thin filaments. In these myofibrils stretched beyond overlap, neither cross-bridges nor ECM can contribute to the change in stiffness upon Ca^{2+} activation. Powers et al. (2014) observed an ∼4-fold increase in myofibril stiffness upon Ca^{2+} activation, which they attributed to activation of titin by some as-yet-unidentified mechanism(s). Their results are similar to the ∼3-fold increase in stiffness that we observed in intact soleus muscles during rapid unloading.

Studies have consistently shown that muscle stiffness increases with force development, presumably owing to the increase in number of attached cross-bridges with increasing muscle activation (Campbell and Moss, 2002). The observed increase in the elastic modulus upon activation during rapid unloading suggests that the stiffness of elastic elements increases proportionally with cross-bridge stiffness in active muscles, perhaps to more effectively transmit the increasing cross-bridge forces to the Z-lines, costameres, and ultimately to muscle tendons (Horowits et al., 1986).

It important to note that there are also differences between myofibril and whole-muscle experiments. Powers et al. (2014, 2016) conducted their experiments on myofibrils obtained from psoas muscles. Psoas muscles are known to have a shorter titin isoform and higher passive tension than soleus muscles (Prado et al., 2005). In addition, Powers et al. (2014, 2016) stretched single myofibrils to compare differences in muscle stiffness, whereas we measured the elastic modulus of active and passive muscles during unloading. In both passive and active muscles, force tends to change non-linearly with muscle length during unloading in contrast to a more linear relationship during stretch (see e.g. Lopez et al., 2008 for data from *mdm* diaphragm). Whereas myofibrils are highly reduced preparations in which the ECM and sarcolemmal structures have been removed, whole muscles include additional structures that might contribute to passive and active muscle stiffness.

Contribution of elastic elements to active and passive muscle stiffness

We used load-clamp experiments to investigate the effects of activation on the stiffness of elastic elements in muscle by measuring elastic recoil during rapid unloading. The cross-bridges themselves are unlikely to contribute to stiffness during rapid unloading because the shortening velocity greatly exceeds maximum contraction velocity (V_{max}) under these conditions. Because only a small number of cross-bridges are attached at a given time at V_{max} (Finer et al., 1995; Stehle and Brenner, 2000), it seems that any cross-bridges that did attach during rapid unloading would detach rapidly without hydrolyzing ATP (Brenner, 1991), and would therefore have a minimal effect on muscle stiffness. Cross-bridges that were already attached when the muscles were initially unloaded (Huxley, 1974), as well as the filament lattice (Kojima et al., 1994; Wakabayashi et al., 1994), would be expected to recoil by only ∼1% of muscle length.

If the initial stress and the change in stress for each muscle are the same in active and passive load-clamp tests, then the recoil of linear elastic elements outside the sarcomere must necessarily also be equivalent. This procedure will eliminate the contribution of any linear elastic elements outside the sarcomere, regardless of magnitude, because the stiffness of linear elements is independent of their initial length. The contribution of non-linear parallel elastic elements in the extracellular matrix cannot be ruled out entirely, because their stiffness does depend on the initial length. To estimate the contribution of extracellular elastic elements to elastic recoil of intact soleus muscles, we conducted load-clamp experiments starting at very short muscle lengths (85% L_0), at which these elements are completely unloaded (Berquin et al., 1994).

In our experiments, wild-type muscles were activated to ∼30% P_0 prior to rapid unloading, whereas passive muscles were stretched by up to 17% L_0 to achieve the same initial force. If the ECM behaves like a parallel non-linear spring, then elastic elements outside the sarcomere could potentially contribute more to elastic recoil in the stretched passive muscle than in the same active muscle at L_0. This effect, if present, would tend to reduce the observed change in stiffness upon activation. In addition, if the ECM is strained during activation at L_0 and contributes to active recoil in the load clamp tests, then shortening the muscle to 85% L_0 should unload the ECM and reduce its contribution to elastic recoil. The observation that there was no difference in elastic recoil between active wild-type muscles recoiling from L_0 and 85% L_0 strongly suggests that there is no measurable contribution of the ECM to elastic recoil at L_0. *mdm* muscles showed a nearly significant effect of length on the stress–strain relationship, likely due to the fact that it was difficult to match the initial forces at 85% L_0 and L_0 in the load-clamp tests.

Although collagen fibers in the endomysium have been observed to reorient modestly upon stretch and shortening of passive muscle in previous studies (Trotter and Purslow, 1992), the associated force has not been measured. Recent models based on passive material properties of porcine muscle suggest that the contribution of stretched parallel elastic elements to passive stiffness becomes significant only at sarcomere lengths longer than those used in our study (Gindre et al., 2013). As a consequence of constant volume, muscles also expand radially during shortening or compression. Radial expansion will also load collagen fibers in the extracellular matrix. However, the increase in stress of collagen fibers due to radial expansion becomes significant only at sarcomere lengths much shorter than the ones used in this study (Gindre et al., 2013).

In summary, our results suggest a negligible contribution of non-linear parallel elastic elements to the observed increase in stiffness and decrease in rest length in active versus passive soleus muscles during unloading. Based on these considerations and Powers et al.'s (2014, 2016) results from single psoas myofibrils, we believe that our results strongly suggest that titin activation contributes to active muscle stiffness, and that its contribution can be measured from intact muscles using load-clamp tests.

Journal of Experimental Biology (2017) 220, 828-836 doi:10.1242/jeb.139717

Titin activation and the *mdm* mutation

In contrast to wild-type muscles, intact *mdm* soleus muscles showed no effect of activation on the length at which elastic elements develop force, or on the slope of the elastic modulus versus stress. Powers et al. (2016) also observed no difference in stiffness between active and passive single myofibrils of *mdm* psoas stretched beyond overlap of the thick and thin filaments. In addition, the decreased stiffness of active *mdm* muscles is quantitatively consistent with the 10-fold lower frequency of tremor during shivering thermogenesis in *mdm* mice (Taylor-Burt et al., 2015). Together with Powers et al.'s (2016) results, our observations suggest the hypothesis that a region of titin, missing in *mdm* muscles, is responsible for increasing titin and muscle stiffness upon activation. However, both decreased maximum isometric force and fibrosis of *mdm* muscles (Lopez et al., 2008) are potentially confounding factors.

Like Lopez et al. (2008) in *mdm* diaphragm, we observed that maximum isometric force is reduced in *mdm* soleus compared with wild-type (Fig. 1A,B). Powers et al. (2016) also observed that force was decreased in single myofibrils of *mdm* psoas compared with wild-type. In psoas myofibrils, the decrease in force was not due to a decrease in myosin or actin content of the myofibrils (Powers et al., 2016). In the experiments reported here, we attempted to account for the difference in maximum stress between genotypes by decreasing activation of wild-type muscles to 30% P_0 so that wild-type and *mdm* muscles were activated to the same initial stress (Fig. 4A,C). Even at only 30% of P_0, wild-type soleus muscles exhibited a substantial increase in stiffness upon activation that was completely absent in *mdm* soleus muscles activated to the same initial stress. Like Powers et al. (2016), we suggest that titin activation fails to occur in *mdm* muscles.

Classic experiments by Horowits et al. (1986) suggest that titin alone in muscle sarcomeres is responsible for transmitting active force from the cross-bridges to the Z-disk. They used radiation to break titin filaments and electron microscopy to show that damage to titin results in a reduction of active tension in skinned single fibers, as well as axial misalignment of thick filaments. Horowits and Podolsky (1987) and Horowits and colleagues (1989) also showed that without force transmission by titin, force generation by the cross-bridges is highly inefficient because energy from cross-bridge interactions is lost to thick filament displacement at the expense of longitudinal tension. Numerous other studies also show that changes in titin isoforms and consequent changes in titin-based stiffness are associated with changes in force production (Ottenheijm et al., 2012; Pulcastro et al., 2016). We suggest that the force deficit in *mdm* muscles is due to impaired transmission of force from the cross-bridges to the Z-lines.

We found that intact *mdm* soleus muscles are passively stiffer during unloading than muscles from wild-type littermates (see Fig. 1B). Lopez et al. (2008) also reported that passive stiffness was higher in the intact diaphragm of *mdm* mice. In contrast, Witt et al. (2004) reported no difference in passive tension of muscle strips from *mdm* soleus, and Powers et al. (2016) reported no differences in passive tension in myofibrils from *mdm* psoas. Diaphragm muscles from *mdm* mice have increased perimysial collagen (Lopez et al., 2008) and it might be that the higher passive tension of soleus muscles reported here is due at least in part to fibrosis, especially because no difference in passive tension was found between genotypes in psoas myofibrils, in which the extracellular matrix is largely absent (Powers et al., 2016).

An increase in stiffness of non-linear parallel elastic elements due to fibrosis is expected to shift the passive stress–strain relationship during unloading to the left, as observed in the present study, potentially decreasing the difference between the passive and active stress–strain curves. It seems unlikely, however, that this increase in passive tension due to fibrosis would completely eliminate the increase in active stiffness during rapid unloading observed in wild-type muscles activated to the same initial force. The passive stress–strain relationship of *mdm* muscles was shifted leftward only slightly compared with passive wild-type muscles. Indeed, the active stiffness is substantially lower in *mdm* soleus than in wild-type soleus (Fig. 4B, D) despite the higher passive tension in *mdm*. Results from load-clamp experiments at 85% L_0 and L_0 further support the idea that ECM does not contribute to elastic recoil at these lengths.

A role for titin in active muscle stiffness

For more than a decade, it has been hypothesized that titin could play a role not only in passive force generation, but also in active skeletal muscle contraction (Reich et al., 2000; Tatsumi et al., 2001; Bagni et al., 2002, 2004; Nishikawa et al., 2012; Rassier et al., 2015). Recently, Leonard and Herzog (2010) and Powers et al. (2014) demonstrated that titin stiffness increases in Ca^{2+}-activated myofibrils stretched beyond overlap of the thick and thin filaments, compared with non-activated myofibrils. They further demonstrated: (1) that mild trypsin digestion, which cleaves titin, completely eliminates the force in response to stretch; and (2) that myofibrils activated on the descending limb of the force–length curve show a smaller increase in stiffness in response to stretch, suggesting that the increase in titin-based stiffness depends on force development.

The increasing acceptance of the idea that titin plays a role in active muscle has led to a proliferation of hypotheses for physiological mechanisms. These include hypotheses that refolding of unfolded Ig domains might increase the speed of muscle shortening (Rivas-Pardo et al., 2016), to the idea that the PEVK region of titin sticks to thin filaments (Rode et al., 2009), and the suggestion that the cross-bridges not only translate but also rotate the thin filaments, thereby winding titin upon them (Nishikawa et al., 2012).

Leonard and Herzog (2010) and others (Herzog et al., 2012, 2016; Monroy et al., 2012; Nishikawa et al., 2012; Rassier et al., 2015) have speculated that the increase in titin-based stiffness upon muscle activation might be due to titin binding to actin or thin filaments. Kellermayer and Granzier (1996) demonstrated that I-band titin from skeletal muscle decreased thin filament motility *in vitro*, but the biochemical basis for the interaction remains to be elucidated. Labeit et al. (2003) suggested that glutamate-rich motifs in the PEVK region of titin bind Ca^{2+}, and increase titin-based stiffness. It is possible that the *mdm* deletion decreases active muscle stiffness by reducing or eliminating Ca^{2+} binding to titin; however, although binding of Ca^{2+} to titin has been shown to increase titin stiffness (Labeit et al., 2003; Joumaa et al., 2008; DuVall et al., 2013), this effect alone is too small to account for the observed increase in stiffness upon activation (Leonard and Herzog, 2010). Recent antibody labeling studies in passive versus active myofibrils demonstrate that extension of titin segments changes upon activation, supporting the hypothesis that interactions between titin and thin filaments might increase active muscle stiffness (Herzog et al., 2016). Further studies are needed to determine how Ca^{2+}–titin–actin interactions affect whole muscle function.

The *mdm* mutation is characterized by a 779 bp deletion in the *Ttn* gene, resulting in a putative 83 amino acid deletion in the N2A region of the protein. It has been suggested that the N2A region of titin is an ideal location for modulating titin stiffness upon muscle activation (Nishikawa et al., 2012), because binding to actin at this location would eliminate low-force straightening of the proximal tandem Ig domains of titin and engage the PEVK region, which extends at much

higher force. We suggest that the *mdm* deletion might eliminate Ca^{2+}-dependent binding of titin to actin at the N2A region or elsewhere, thereby preventing the increase in titin stiffness upon activation.

Because the 83 amino acid deletion in *mdm* is predicted to have a negligible effect on titin stiffness owing to the change in protein size alone, it was suggested that the *mdm* mutation might lead indirectly to a decrease in PEVK domain repeats via post-transcriptional processing (Lopez et al., 2008) or to the induction of CARP expression, which might bind to N2A and affect myofibrillar signaling (Witt et al., 2004). In fact, a recent study on mice with a deletion of Ig domains 3–11 near the Z-line demonstrated differential splicing of PEVK and other regions of the titin protein, which led to increased passive stiffness of intact soleus muscles (Buck et al., 2014). Owing to the likelihood of post-transcriptional processing of titin in *mdm* muscles, it is possible that impaired titin activation might occur as a result of skipped exons rather than as a result of the primary N2A deletion.

Conclusion

In summary, the results of this study demonstrate that activation of titin, an elastic element within muscle sarcomeres, can be observed in intact muscles using load-clamp tests, despite the potentially confounding effects of the extracellular matrix and other elastic structures. The results that we obtained here are qualitatively and quantitatively similar to results obtained in single myofibrils from wild-type and *mdm* mouse psoas by Powers et al. (2014, 2016). In these studies, Powers et al. (2014) found that the stiffness of wild-type psoas myofibrils increased ∼4-fold upon activation. Powers et al. (2016) further demonstrated that myofibrils from *mdm* psoas exhibit a deficit in titin-based active force.

These results are consistent with the idea that, in addition to the thin filaments, titin is activated by Ca^{2+} influx in skeletal muscle (Leonard and Herzog, 2010; Nishikawa et al., 2012). The results also suggest that the mechanism of titin activation is impaired in skeletal muscles from *mdm* mice, which carry a deletion in the N2A region of titin. Although it is possible that the N2A region of titin binds to thin filaments to increase titin stiffness, a deletion in some other part of the titin protein, due to post-transcriptional processing, cannot be ruled out at this time. In the future, antibody labeling and biochemistry of the N2A region in wild-type and *mdm* muscles will be crucial for understanding the mechanisms of titin activation by Ca^{2+} in skeletal muscle (Granzier, 2010).

Acknowledgements

The authors wish to thank Stan Lindstedt, Walter Herzog and Thomas Sandercock for their insightful comments on previous versions of the manuscript.

Competing interests

The authors declare no competing or financial interests.

Author contributions

J.A.M.: data collection, analysis and interpretation, paper preparation and editing; K. L.P.: data collection; C.M.P.: mouse genotyping; T.U.: data analysis and programming; K.C.N.: conceptual development, funding, interpretation and editing.

Funding

This work was supported by National Science Foundation grants IOS-1025806, IOS-1456868; and an award from the W. M. Keck Foundation.

References

Akimoto, T. and Sugi, H. (1999). Structural origin of the series elastic component in horseshoe crab skeletal muscle fibers. *Comp. Biochem. Physiol.* **122A**, 139-144.

Askew, G. N. and Marsh, R. L. (1997). The effects of length trajectory on the mechanical power output of mouse skeletal muscles. *J. Exp. Biol.* **200**, 3119-3131.

Bagni, M. A., Cecchi, G., Colombini, B. and Colomo, F. (2002). A non-cross-bridge stiffness in activated frog muscle fibers. *Biophys. J.* **82**, 3118-3127.

Bagni, M. A., Colombini, B., Geiger, P., Belinguer Palmini, R. and Cecchi, G. (2004). Non-cross-bridge calcium-dependent stiffness in frog muscle fibers. *Am. J. Physiol. Cell Physiol.* **286**, C1353-C1357.

Berquin, A., Schmit, P., Moens, P. and Lebacq, J. (1994). Compliance of normal, dystrophic and transplanted mouse muscles. *J. Biomech.* **27**, 1331-1337.

Brenner, B. (1991). Rapid dissociation and reassociation of actomyosin cross-bridges during force generation: A newly observed facet of cross-bridge action in muscle. *Proc. Natl. Acad. Sci. USA* **88**, 10490-10494.

Buck, D., Smith, J. E., Chung, C. S., Ono, Y., Sorimachi, H., Labeit, S. and Granzier, H. L. (2014). Removal of immunoglobulin-like domains from titin's spring segment alters titin splicing in mouse skeletal muscle and causes myopathy. *J. Gen. Physiol.* **143**, 215-230.

Burkholder, T. J. and Lieber, R. L. (2001). Sarcomere length operating range of vertebrate muscles during movement. *J. Exp. Biol.* **204**, 1529-1536.

Burkholder, T. J., Fingado, B., Baron, S. and Lieber, R. L. (1994). Relationship between muscle fiber types and sizes and muscle architectural properties in the mouse hindlimb. *J. Morphol.* **221**, 177-190.

Campbell, K. S. and Moss, R. L. (2002). History-dependent mechanical properties of permeabilized rat soleus muscle fibers. *Biophys. J.* **82**, 929-943.

DuVall, M. M., Gifford, J. L., Amrein, M. and Herzog, W. (2013). Altered mechanical properties of titin immunoglobulin domain 27 in the presence of calcium. *Eur. Biophys. J.* **42**, 301-307.

Finer, J. T., Mehta, A. D. and Spudich, J. A. (1995). Characterization of single actin-myosin interactions. *Biophys. J.* **68**, 291S-296S.

Garvey, S. M., Rajan, C., Lerner, A. P., Frankel, W. N. and Fox, G. A. (2002). The muscular dystrophy with myositis (*mdm*) mouse mutation disrupts a skeletal muscle-specific domain of titin. *Genomics* **79**, 146-149.

Gindre, J., Takaza, M., Moerman, K. M. and Simms, C. K. (2013). A structural model of passive skeletal muscle shows two reinforcement processes in resisting deformation. *J. Mech. Behav. Biomed. Mater.* **22**, 84-94.

Goulding, D., Bullard, B. and Gautel, M. (1997). A survey of in situ sarcomere extension in mouse skeletal muscle. *J. Muscle Res. Cell Motil.* **18**, 465-472.

Granzier, H. L. (2010). Activation and stretch-induced passive force enhancement —are you pulling my chain? Focus on "Regulation of muscle force in the absence of actin-myosin-based cross-bridge interaction". *Am. J. Physiol. Cell Physol.* **299**, C11-C13.

Herzog, W. and Leonard, T. R. (2002). Force enhancement following stretching of skeletal muscle: a new mechanism. *J. Exp. Biol.* **205**, 1275-1283.

Herzog, W., Leonard, T. R., Joumaa, V., DuVall, M. and Panchangam, A. (2012). The three filament model of skeletal muscle stability and force production. *Mol. Cell. Biomech.* **9**, 175-191.

Herzog, W., Schappacher, G., DuVall, M., Leonard, T. R. and Herzog, J. A. (2016). Residual force enhancement following eccentric contractions: A new mechanism involving titin. *Physiology* **31**, 300-312.

Horowits, R. and Podolsky, R. J. (1987). The positional stability of thick filaments in activated skeletal muscle depends on sarcomere length: Evidence for the role of titin filaments. *J. Cell Biol.* **105**, 2217-2223.

Horowits, R., Kempner, E. S., Bisher, M. E. and Podolsky, R. J. (1986). A physiological role for titin and nebulin in skeletal muscle. *Nature* **323**, 160-164.

Horowits, R., Maruyama, K. and Podolsky, R. J. (1989). Elastic behavior of connectin filaments during thick filament movement in activated skeletal muscle. *J. Cell Biol.* **109**, 2169-2176.

Huebsch, K. A., Kudryashova, E., Wooley, C. M., Sher, R. B., Seburn, K. L., Spencer, M. J. and Cox, G. A.. (2005). Mdm muscular dystrophy: interactions with calpain 3 and a novel functional role for titin's N2A domain. *Hum. Mol. Genet.* **14**, 2801-2811.

Huxley, A. F. (1974). Muscular contraction. *J. Physiol.* **243**, 1-43.

James, R. S., Tallis, J. and Angilletta, M. J.Jr. (2015). Regional thermal specialisation in a mammal: temperature affects power output of core muscle more than that of peripheral muscle in adult mice (*Mus musculus*). *J. Comp. Physiol. B.* **185**, 135-142.

Jewell, B. R. and Wilkie, D. R. (1958). An analysis of the mechanical components in frog's striated muscle. *J. Physiol.* **143**, 515-540.

Joumaa, V. V., Leonard, T. R. and Herzog, W. (2008). Residual force enhancement in myofibrils and sarcomeres. *Proc. R. Soc. B Biol. Sci.* **275**, 1411-1419.

Kellermayer, M. S. Z. and Granzier, H. L. (1996). Calcium-dependent inhibition of *in vitro* thin-filament motility by native titin. *FEBS Lett.* **380**, 281-286.

Kojima, H., Ishijima, A. and Yanagida, T. (1994). Direct measurement of stiffness of single actin filaments with and without tropomyosin by in vitro nanomanipulation. *Proc. Natl. Acad. Sci. USA* **91**, 12962-12966.

Labeit, D., Watanabe, K., Witt, C., Fujita, H., Wu, Y., Lahmers, S., Funck, T., Labeit, S. and Granzier, H. (2003). Calcium-dependent molecular spring elements in the giant protein titin. *Proc. Natl. Acad. Sci. USA* **100**, 13716-13721.

Lappin, A. K., Monroy, J. A., Pilarski, J. Q., Zepnewski, E. D., Pierotti, D. J. and Nishikawa, K. C. (2006). Storage and recovery of elastic potential energy powers ballistic prey capture in toads. *J. Exp. Biol.* **209**, 2535-2553.

Leonard, T. R. and Herzog, W. (2010). Regulation of muscle force in the absence of actin-myosin-based cross-bridge interaction. *Am. J. Physiol. Cell Physiol.* **299**, C14-C20.
Lindstedt, S. L., Reich, T. E., Keim, P. and LaStayo, P. C. (2002). Do muscles function as adaptable locomotor springs? *J. Exp. Biol.* **205**, 2211-2216.
Linke, W. A., Ivemeyer, M., Mundel, P., Stockmeier, M. R. and Kolmerer, B. (1998). Nature of PEVK-titin elasticity in skeletal muscle. *Proc. Natl. Acad. Sci. USA* **95**, 8052-8057.
Lopez, M. A., Pardo, P. S., Cox, G. A. and Boriek, A. M. (2008). Early mechanical dysfunction of the diaphragm in the muscular dystrophy with myositis (Ttn-mdm) model. *Am. J. Physiol. Cell Physiol.* **295**, C1092-C1102.
Magid, A. and Law, D. J. (1985). Myofibrils bear most of the resting tension in frog skeletal muscle. *Science* **230**, 1280-1282.
Maruyama, K. (1976). Connectin, an elastic protein from myofibrils. *J. Biochem.* **80**, 405-407.
Maxwell, L. C., Faulkner, J. A. and Hyatt, G. J. (1974). Estimation of number of fibers in guinea pig skeletal muscles. *J. Appl. Physiol.* **37**, 259-264.
Monroy, J. A., Lappin, A. K. and Nishikawa, K. C. (2007). Elastic properties of active muscle-on the rebound? *Exerc. Sports Sci. Rev.* **35**, 174-179.
Monroy, J. A., Powers, K. L., Gilmore, L. A., Uyeno, T. A., Lindstedt, S. L. and Nishikawa, K. C. (2012). What is the role of titin in active muscle? *Exerc. Sports. Sci. Rev.* **40**, 73-78.
Nishikawa, K. C., Monroy, J. A., Uyeno, T. E., Yeo, S. H., Pai, D. K. and Lindstedt, S. L. (2012). Is titin a 'winding filament'? A new twist on muscle contraction. *Proc. R. Soc. Lond. B Biol. Sci.* **279**, 981-990.
Ottenheijm, C. A. C., Voermans, N. C., Hudson, B. D., Irving, T., Stienen, G. J. M., van Engelen, B. G. and Granzier, H. (2012). Titin-based stiffening of muscle fibers in Ehlers-Danlos Syndrome. *J. Appl. Physiol.* **112**, 1157-1165.
Powers, K., Schappacher-Tilp, G., Jinha, A., Leonard, T., Nishikawa, K. and Herzog, W. (2014). Titin force is enhanced in actively stretched skeletal muscle. *J. Exp. Biol.* **217**, 3629-3636.
Powers, K., Nishikawa, K., Joumaa, V. and Herzog, W. (2016). Decreased force enhancement in skeletal muscle sarcomeres with a deletion in titin. *J. Exp. Biol.* **219**, 1311-1316.
Prado, L. G., Makarenko, I., Andresen, C., Krüger, M., Opitz, C. A. and Linke, W. A. (2005). Isoform diversity of giant proteins in relation to passive and active contractile properties of rabbit skeletal muscles. *J. Gen. Physiol.* **126**, 461-480.
Pulcastro, H. C., Awinda, P. O., Methawasin, M., Granzier, H., Dong, W. and Tanner, B. C. W. (2016). Increased Titin Compliance Reduced Length-dependent contraction and slowed cross-bridge kinetics in skinned myocardial strips from Rbm20ΔRRM mice. *Front. Physiol.* **7**, 322.
Rassier, D. E., Leite, F. S., Nocella, M., Cornachione, A. S., Colombini, B. and Bagni, M. A. (2015). Non-crossbridge forces in activated striated muscles: a titin dependent mechanism of regulation. *J. Muscle Res. Cell Motil.* **36**, 37-45.
Reich, T. E., Lindstedt, S. L., LaStayo, P. C. and Pierotti, D. J. (2000). Is the spring quality of muscle plastic? *Am. J. Physiol. Regul. Integr. Comp. Physiol.* **278**, R1661-R1666.
Rivas-Pardo, J. A., Eckels, E. C., Popa, I., Kosuri, P., Linke, W. A. and Fernández, J. M. (2016). Work done by titin protein folding assists muscle contraction. *Cell Rep.* **14**, 1339-1347.
Roberts, T. J. (2016). Contribution of elastic tissues to the mechanics and energetics of muscle function during movement. *J. Exp. Biol.* **219**, 266-275.
Rode, C., Siebert, T. and Blickhan, R. (2009). Titin-induced force enhancement and force depression: a 'sticky-spring' mechanism in muscle contractions? *J. Theor. Biol.* **259**, 350-360.
Sacks, R. D. and Roy, R. R. (1982). Architecture of the hind limb muscles of cats: functional significance. *J. Morphol.* **173**, 185-195.
Stehle, R. and Brenner, B. (2000). Cross-bridge attachment during high-speed active shortening of skinned fibers of the rabbit psoas muscle: implications for cross-bridge action during maximum velocity of filament sliding. *Biophys. J.* **78**, 1458-1473.
Sugi, H., Akimoto, T., Kobayashi, T., Suzuki, S. and Shimada, S. (2000). Possible contribution of titin filaments to the compliant series elastic component in horseshoe crab skeletal muscle fibers. *Adv. Exp. Med. Biol.* **481**, 371-380.
Tatsumi, R., Maeda, K., Hattori, A. and Takahashi, K. (2001). Calcium binding to an elastic portion of connectin/titin filaments. *J. Muscle Res. Cell Motil.* **22**, 149-162.
Trotter, J. A. and Purslow, P. P. (1992). Functional morphology of the endomysium in series fibered muscles. *J. Morphol.* **212**, 109-122.
Taylor-Burt, K. R., Monroy, J., Pace, C., Lindstedt, S. and Nishikawa, K. C. (2015). Shiver me titin! Elucidating titin's role in shivering thermogenesis. *J. Exp. Biol.* **218**, 694-702.
Wakabayashi, K., Sugimoto, Y., Tanaka, H., Ueno, Y., Takezawa, Y. and Amemiya, Y. (1994). X-ray diffraction evidence for the extensibility of actin and myosin filaments during muscle contraction. *Biophys. J.* **67**, 2422-2435.
Wang, K., McCarter, R., Wright, J., Beverly, J. and Ramirez-Mitchell, R. (1991). Regulation of skeletal muscle stiffness and elasticity by titin isoforms: a test of the segmental extension model of resting tension. *Proc. Natl. Acad. Sci. USA* **88**, 7101-7105.
Wilkie, D. R. (1956). The mechanical properties of muscle. *Brit. Med. Bull.* **12**, 177-182.
Witt, C. C., Ono, Y., Puschmann, E., McNabb, M., Wu, Y., Gotthardt, M., Witt, S. H., Haak, M., Labeit, D., Gregorio, C. C. et al. (2004). Induction and myofibrillar targeting of CARP, and suppression of the Nkx2.5 pathway in the *mdm* mouse with impaired titin-based signaling. *J. Mol. Biol.* **336**, 145-154.

Journal of Experimental Biology